

1 **Apixaban, an orally available anticoagulant, inhibits SARS-CoV-2**
2 **replication by targeting its major protease in a non-competitive way**

3

4 Otávio Augusto Chaves,^{1,2,*} Carolina Q. Sacramento,^{1,2} Natalia Fintelman-Rodrigues,^{1,2}
5 Jairo Ramos Temerozo,^{3,4} Filipe Pereira-Dutra,¹ Daniella M. Mizurini,⁵ Robson Q.
6 Monteiro,⁵ Leonardo Vazquez,^{1,2} Patricia T. Bozza¹, Hugo Caire Castro-Faria-Neto,¹
7 Thiago Moreno L. Souza,^{1,2,*}

8

9 ¹ *Laboratory of Immunopharmacology, Oswaldo Cruz Institute (IOC), Oswaldo Cruz*
10 *Foundation (Fiocruz), Rio de Janeiro, RJ, Brazil.*

11 ² *National Institute for Science and Technology on Innovation on Neglected Diseases*
12 *(INCT/IDN), Center for Technological Development in Health (CDTS), Oswaldo Cruz*
13 *Foundation (Fiocruz), Rio de Janeiro, RJ, Brazil.*

14 ³ *National Institute for Science and Technology on Neuroimmunomodulation*
15 *(INCT/NIM), Oswaldo Cruz Institute (IOC), Oswaldo Cruz Foundation (Fiocruz), Rio*
16 *de Janeiro, RJ, Brazil.*

17 ⁴ *Laboratory on Thymus Research, Oswaldo Cruz Institute (IOC), Oswaldo Cruz*
18 *Foundation (Fiocruz), Rio de Janeiro, RJ, Brazil.*

19 ⁵ *Institute of Medical Biochemistry Leopoldo de Meis, Federal University of Rio de*
20 *Janeiro (UFRJ), Rio de Janeiro, RJ, Brazil.*

21

22

23

24

25

26

27

28 *Corresponding authors: otavioaugustochaves@gmail.com (O.A.C.) and
29 tmoreno@cdts.fiocruz.br (T.M.L.S.).

30

31 **Abstract**

32 Anticoagulants are associated with clinical benefit against the 2019 coronavirus
33 disease (COVID-19), preventing COVID-19 associated coagulopathy. Blood
34 coagulation factor Xa (FXa) and SARS-CoV-2 major protease (M^{Pro}) share over 80%
35 homology at the three-dimensional protein level. Thus, it is worth interrogating whether
36 there is crosstalk between inhibitors and substrates between these enzymes. Here, we
37 found that the clinically-approved FXa inhibitor apixaban targets SARS-CoV-2 M^{Pro}
38 with a 21-fold higher potency than boceprevir (GC376). Apixaban displayed a non-
39 competitive mechanism of inhibition towards M^{Pro}, since it targets the enzyme/substrate
40 complex and the allosteric site onto the viral protease. Enzymatic assays were further
41 validated in infected Calu-3 cells, which reveal that apixaban decreases the production
42 of infectious viral particles in a dose-dependent manner, with an inhibitory potency in
43 the micromolar range. Our results are in line with the proposed early use of
44 anticoagulants, including FXa inhibitors, to improve clinical outcome of COVID-19
45 patients. In this context, apixaban may display a dual mechanism of action by targeting
46 FXa to prevent coagulopathy and, at some level, SARS-CoV-2 M^{Pro}.

47
48
49

50 **Keywords:** SARS-CoV-2, apixaban, rivaroxaban, dabigatran, proteases, repurposing
51 drugs.

52

53 Introduction

54 The severe acute respiratory syndrome coronavirus 2 (SARS-CoV-2), the
55 etiological agent of 2019 coronavirus disease 2019 (COVID-19), causes asymptomatic
56 to life-threatening conditions, leaving 4.5 million deaths globally from January 2020 to
57 August 2021^{1,2}. Before reaching the severity of disease – characterized by acute
58 respiratory failure, hyper-inflammation, and coagulopathy – early increase in blood
59 levels of C reactive protein (CRP) and D-dimer already suggest poor clinical
60 progression in COVID-19 patients^{3,4}.

61 High D-dimer levels in COVID-19 patients are the final product of the
62 hyperactivated clotting/fibrinolysis pathways and coagulation factor Xa (FXa)
63 engagement is a key and rate-limiting event along with thrombin and fibrin
64 generation^{5,6}. These vascular changes in COVID-19 patients are enhanced by the pro-
65 inflammatory cytokine storm that increases vascular permeability⁷. In fact, both
66 cytokine storm and coagulopathy are triggered by the virus, as exemplified by
67 monocytes from critically ill COVID-19 patients that expose tissue factor (CD142), a
68 clotting trigger⁸. SARS-CoV-2 replication in type II pneumocytes leads to diffuse
69 alveolar damage, and along with the formation of fibrin, documented in the necropsy
70 of COVID-19 patients^{5,9}, which may reduce alveolar hematosis.

71 Since the SARS-CoV-2 outbreak, the use of anticoagulants became part of the
72 standard care in the management of COVID-19 patients¹⁰⁻¹³. Either broad and specific
73 anticoagulants such as low-molecular weight heparin, direct thrombin/FXa inhibitors,
74 and warfarin were recommended in the 2021 guidelines by both the American Society
75 of Hematology (ASH) and National Institutes of Health (NIH) to critical and
76 hospitalized patients¹⁴⁻¹⁸. Nevertheless, the posology of anticoagulants for COVID-19
77 patients may require adjustments; because current doses and regimens were imported
78 from general practice to treat thrombosis and/or embolism¹⁹. Under these recently
79 adapted conditions, antithrombotic treatment has been associated with decreased
80 mortality in COVID-19 patients^{16,18,20,21}; thus, confirming coagulopathy is a central
81 event in the physiopathology of COVID-19.

82 The main protease (M^{Pro}) of SARS-CoV-2 is considered as one of the main
83 targets for drug repurposing, due to its cleavage activity at eleven sites at the viral
84 polyprotein²². Curiously, FXa and thrombin share a considerable similarity to SARS-
85 CoV-2 M^{Pro} binding site (according to the respective dimensionless scores of 0.71 and

86 0.74, in a maximum of 1.00). Compared to SARS-CoV-2 M^{pro}, FXa and thrombin
87 superpose their three-dimensional structures with a minor differences, with respect to
88 Root Mean Square Deviation (RMSD) analysis of just 2.57 and 2.49 Å,
89 respectively^{22,23}. Although structural similarities between FXa and thrombin with M^{pro}
90 have been suggested, functional studies to indicate whether M^{pro} could use FXa and
91 thrombin inhibitors or substrates are scarce. Here, we demonstrated that the direct FXa
92 inhibitor apixaban blocks SARS-CoV-2 M^{pro} enzymatic activity in a non-competitive
93 way. As a consequence, apixaban impairs SARS-CoV-2 replication in a dose-dependent
94 manner in human lung epithelial (Calu-3) cells.

95

96 **Results**

97 *Apixaban non-competitively inhibits SARS-CoV-2 M^{pro}*

98 The FXa and thrombin show considerable similarity to M^{pro} binding site, as
99 judged by the 3D superimposition of their structures with a good correlation (Fig. 1A)
100 and in line with previous literature^{22,23}. Thus, we interrogated if the M^{pro} (and as a
101 control papain-like protease, PL^{pro}) was susceptible to direct inhibitors of FXa
102 (apixaban and rivaroxaban) and thrombin (dabigatran). Among the anticoagulants
103 tested, apixaban displayed Morrison's inhibitory constant (K_i) values consistent with
104 inhibition of a good inhibitory profile for M^{pro}, but not for PL^{pro} (Fig. 1B and C). No
105 compound inhibited PL^{pro} better than the positive control GRL0617 (Fig. 1B). With
106 respect to the M^{pro}, apixaban was 21-fold more potent than the positive controls
107 boceprevir (GC376) and atazanavir, both on clinical trials against COVID-19 (Fig. 1C).
108 Of note, the FXa inhibitor, ribaroxaban and the thrombin inhibitor, dabigatran were as
109 potent as boceprevir (Fig. 1C).

110 Since apixaban inhibits M^{pro} with a K_i lower than the concentration of the viral
111 protease used in the assay, a non-canonical mechanism of inhibition over this enzyme
112 might be expected. When apixaban's inhibition over M^{pro} was assayed under different
113 concentrations of substrate, a non-competitive mechanism was observed (Fig. 1D). The
114 Michaelis-Menten constant (K_m) value was not altered by apixaban, suggesting M^{pro} is
115 not halted to interact with its substrate by apixaban (Fig. 1D). In addition, there was a
116 significant decrease in the M^{pro} maximum velocity (V_{max}) by apixaban (Fig. 1D),
117 indicating that the enzyme (E) M^{pro} bound to its substrate (S), in the enzyme-substrate
118 complex (ES) and was unable to cleave it and form the products (P) (Fig. 1E).

119 Based on molecular docking, we explored different alternative to explain these
120 results. When interacting with M^{pro}, its peptidic substrate occupies the four enzymatic
121 subsites (S1, S1', S2, and S4) onto the active binding pocket with a docking score
122 (dimensionless) of 65.54 (Fig. 1F). In the M^{pro}/peptide (ES) complex, the substrate
123 forms an external loop, which is targeted by the anticoagulants (Fig. 1G); in particular,
124 apixaban has the most favorable interaction compared with dabigatran and rivaroxaban
125 due to the significant hydrogen bonding interaction with substrate (3.00 Å, Fig. 1G and
126 Supplementary Figs. 2A-C). Moreover, three additional binding pockets in the dimer
127 interface of M^{pro} were identified and associated with allosteric regulation^{24,25}. Molecular
128 docking calculations suggested that apixaban binds onto the allosteric site of M^{pro} with
129 high number of hydrogen bonding and van der Waals interactions (Figs. 1H and 1I).
130 Rivaroxaban did not reach the allosteric site; just the M^{pro}/M^{pro} dimeric interface and
131 dabigatran did not present a feasible binding capacity into these additional sites (Fig. 1H
132 and Supplementary Fig. 2D).

133 Next, we evaluated if whether SARS-CoV-2 proteases could cleave the synthetic
134 chromogenic substrates designed for thrombin (S-2238) and coagulation FXa (S-2765).
135 Despite M^{pro} and FXa similarities described above, the substrates were not cleaved by
136 M^{pro}, nor by PL^{pro}, also included as control (Supplementary Fig. 1A). In fact, host and
137 viral enzymes belong to different families of endopeptidases and M^{pro} lacks the
138 superimposed of random coils that are external of the active site of FXa, which might
139 impact the mimetic chromogenic substrate accommodation into M^{pro} active site (Fig.
140 1A).

141

142 *Apixaban inhibits SARS-CoV-2 replication in a dose-dependent manner in pneumocyte*
143 *cell lineage*

144 To further demonstrate SARS-CoV-2 susceptibility to anticoagulants, Calu-3
145 that recapitulates the most affected cells in the respiratory tract, the type II
146 pneumocytes²⁶, were infected and treated with these compounds. Anticoagulants
147 inhibited the production of infectious SARS-CoV-2 progeny in a dose-dependent
148 manner (Figs. 2A and 2B). Consistently with the enzymatic data, apixaban was
149 approximately 3-fold more potent than any other anti-clotting drugs tested (Table 1).
150 Nevertheless, apixaban was about 5- and 60-fold less potent in vitro in comparison to
151 the positive control atazanavir and remdesivir, respectively (Table 1), indicating that
152 apixaban shows an interestingly scaffold for the design of novel compounds to increase

153 its antiviral action. Despite a slightly higher cytotoxicity, compared to other tested
154 compounds, apixaban's selectivity index (SI) for SARS-CoV-2 replication was two-fold
155 better than other anticoagulants (Table 1). Altogether our results confirm that
156 apixaban's chemical structure is endowed with antiviral activity against SARS-CoV-2.

157

158 **Discussion**

159 Severe COVID-19 could be characterized as a SARS-CoV-2-triggered host-
160 related cytokine storm and coagulopathy²⁷. In this sense, clinical trials have been
161 investigating whether COVID-19 patients could benefit from oral anticoagulant agents,
162 such FXa and thrombin inhibitors¹⁴⁻²¹. Indeed, an increasing body of evidence
163 reinforces that anti-clotting drugs increase the survival probability of critically ill
164 COVID-19 patients under non- and invasive ventilatory assistance^{15,16,18,21,28}. Moreover,
165 other clinical studies also suggest that the early use of anti-thrombotic agents could
166 prevent the consumption of platelets, clotting factors, and ultimately hemorrhagy^{16,19,28}.
167 The high levels of D-dimer, a final product from clotting and fibrinolysis, directly
168 implicate these cascades in the physiopathology of COVID-19²⁸. Thus, the benefit from
169 anticoagulants is well rationalized as host-acting agents. Nevertheless, because of the
170 structural similarities between SARS-CoV-2 M^{pro} and FXa²³, we studied here if: i) M^{pro}
171 could directly cleave FXa substrate, for comparisons we also included PL^{pro} and other
172 substrates in the analysis; ii) FXa inhibitors could also directly target viral M^{pro} and
173 replication, for comparison PL^{pro} and other inhibitors were included. We found that
174 apixaban is a potent M^{pro} inhibitor with a unique mechanism of action and,
175 consequently, reduced SARS-CoV-2 replication.

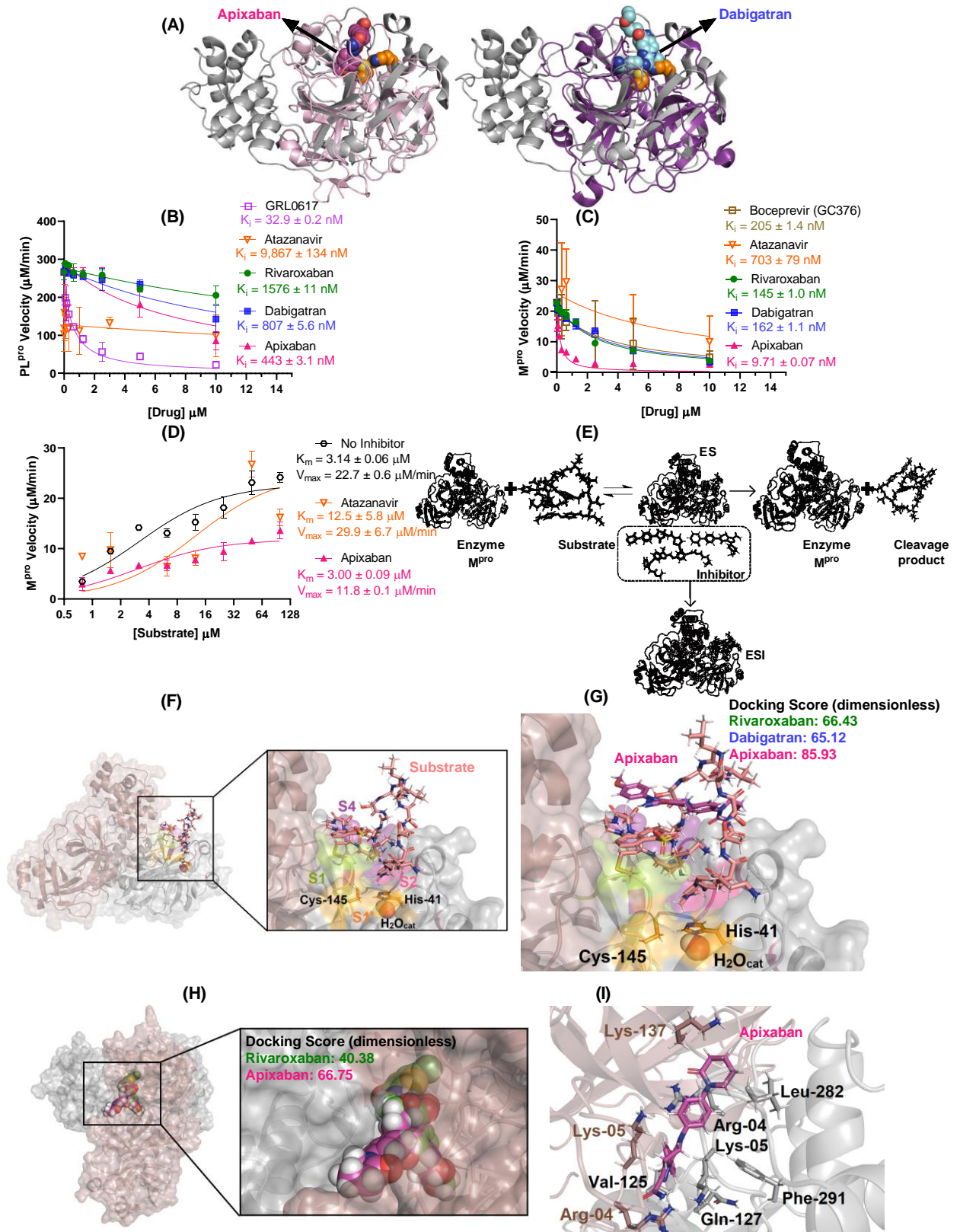
176 Remarkably, the oral anti-factor Xa drug apixaban was a potent M^{pro} inhibitor,
177 comparable to other repurposed drugs on clinical trials against COVID-19, such as the
178 HIV protease inhibitor atazanavir. Differently from atazanavir, apixaban was a non-
179 competitive inhibitor of M^{pro}, targeting the allosteric site of the viral enzyme and its
180 secondary complex bound to the substrate. These characteristics suggest that apixaban
181 chemical structure could be even worth for further hit-to-lead development against
182 COVID-19. The cell-free-based assays were further validated in SARS-CoV-2
183 replicative experiments, confirming that apixaban directly inhibits SARS-CoV-2
184 replication.

185 Under clinically approved posology of 10 mg, apixaban reaches a maximum
186 plasmatic concentration (C_{max}) of 0.55 μM ²⁹. Considering that 87% of the apixaban is

187 bound to albumin³⁰, its free fraction at C_{max} is equivalent to 72 nM, almost 10-times
188 higher than apixaban's K_i towards M^{pro} . On the other side, cell-based assays, display
189 apixaban's potency as 3-times higher than human C_{max} . Despite apixaban is more potent
190 than atazanavir to inhibit M^{pro} , the IC_{50} value for apixaban was not better than
191 atazanavir, probably due to the influence of permeability into the cells: logP for
192 apixaban and atazanavir of 2.71 and 4.50, respectively. These comparisons, of cell-free
193 and -based experiments on the pharmacokinetic parameters lead to paradoxical
194 interpretations on whether apixaban could be acting as a direct acting antivirals in
195 COVID-19 patients. We interpret that cell-based assay conditions are subjected of
196 greater interference than enzymatic experiments. For example, Calu-3 infection was
197 conducted at the considerable multiplicity of infection of 0.1 (1 virus plaque forming
198 unit/10 cells) and cells are maintained with 10% fetal bovine serum, which may bind
199 apixaban. Enzyme kinetic assays were suggestive of a direct acting antiviral activity –
200 which is in line with early clinical use of apixaban during COVID-19^{31,32}.

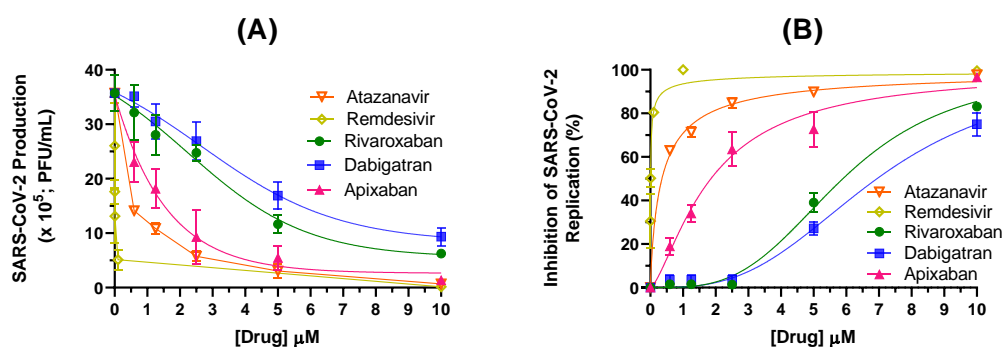
201 It is naturally difficult to estimate a clinical benefit of any antiviral activity of
202 apixaban during clinical trials because its anti-clotting activity is directly associated
203 with COVID-19 physiopathology. Nevertheless, apixaban chemical structure could
204 even be optimized to the development of novel non-competitive M^{pro} inhibitors that
205 preserve anticoagulant activity.

206 Finally, under our experimental conditions, M^{pro} was unable to cleave S-2765, a
207 mimetic chromogenic substrate that recapitulates pro-thrombin cleavage site, possibly
208 due to structural and functional differences between M^{pro} and FXa at the random coil
209 region.



210
 211 **Fig. 1.** (A) Superposition of the monomeric unit of M^{pro} (in gray, PDB code 7K40) with FXa (on the left
 212 in violet, PDB code 2P16) and thrombin (on the right in purple, PDB code 1KTS). The crystallographic
 213 structure of apixaban into FXa structure, dabigatran into thrombin structure, and catalytic dyad of M^{pro}
 214 (His-41 and Cys-145 residues) are as spheres in pink, cyan, and orange, respectively. For better

215 interpretation the catalytic water (H_2O_{cat}) of M^{pro} is not shown. The enzymatic inhibition profile for
 216 apixaban, rivaroxaban, and dabigatran (0, 0.08, 0.16, 0.31, 0.63, 1.25, 2.5, 5.0, and 10 mM) into (B) PL^{pro}
 217 (8.19 nM) and (C) M^{pro} (88.8 nM) velocity. The positive controls GRL0617 (PL^{pro}) and GC376 (M^{pro})
 218 were used under the same condition of anticoagulants. (D) Michaelis-Menten enzymatic mechanism for
 219 M^{pro} without and in the presence of a fixed apixaban or atazanavir concentration (2.5 mM) for different
 220 substrate concentrations (0, 0.76, 1.56, 3.12, 6.25, 12.5, 25.0, 50.0, and 100 mM). (E) Enzymatic scheme
 221 for the experimental mechanism of M^{pro} inhibition by anticoagulants. Best docking pose (ChemPLP
 222 function) for the interaction between M^{pro} (F) substrate, and (G) substrate-apixaban into the active site of
 223 protease. Best docking pose (ChemPLP function) for the interaction between the dimer interface of M^{pro}
 224 (H) apixaban and rivaroxaban, while (I) shows the selected amino acid residues which interact with
 225 apixaban. Substrate, rivaroxaban, dabigatran, and apixaban are in stick representation in beige, green,
 226 cyan, and pink, respectively, while the catalytic water (H_2O_{cat}) is in sphere. Elements' color: hydrogen,
 227 nitrogen, oxygen, sulfur, and chloro are in white, dark blue, red, yellow, and dark green, respectively.



228
 229 **Fig. 2.** Antiviral activity of anticoagulants, atazanavir, and remdesivir in Calu-3 cells (densities of $2.0 \times$
 230 10^5 cells/well) infected with SARS-CoV-2 (MOI 0.1) in 96-well plates. The data is presented as (A) virus
 231 production (PFU/mL) and (B) percentage of viral replication inhibition. The data represent means \pm SEM
 232 of three independent experiments.

233

234 **Table 1.** The 50% effective concentration (EC₅₀ for MOI 0.1), 50% cytotoxic concentration (CC₅₀), and
 235 selectivity index (SI) of the anticoagulants, atazanavir, and remdesivir in Calu-3 cells.

Anticoagulants	EC ₅₀ (μM)	CC ₅₀ (μM)	SI
Atazanavir	0.353 ± 0.018	312 ± 8	884
Remdesivir	0.0305 ± 0.0031	512 ± 30	1.68 × 10 ⁴
Rivaroxaban	5.90 ± 0.30	553 ± 28	93.7
Dabigatran	6.94 ± 0.35	756 ± 38	109
Apixaban	1.84 ± 0.09	491 ± 25	267

236

237 **Methods**

238 *General*

239 All reagents were purchased from Sigma-Aldrich/Merck (St. Louis, MO, USA),
240 HyClone Laboratories Inc. (Logan, Utah) or Chromogenix (Diapharma Group, Inc.,
241 KY). The SARS-CoV-2 virus was isolated from a nasopharyngeal swab of a confirmed
242 case from Rio de Janeiro, Brazil, and its complete genome was sequenced and publicly
243 deposited (GenBank #MT710714; Institutional Review Broad approval,
244 30650420.4.1001.0008).

245

246 *Enzymatic assays*

247 The anticoagulant capacity in inhibit enzymatic activity of M^{pro} and papain-like
248 protease (PL^{pro}) from SARS-CoV-2 were determined by the commercial kit provided by
249 BPS Biosciences® company (catalog number: #79955-1 and #79995-1, respectively)
250 following the procedure and recommendations from literature and company^{33,34}. The
251 enzymatic inhibition was evaluated by varying concentrations of the anti-clotting drugs.
252 Next, the mechanism of inhibition was determined via Michaelis-Menten by varying
253 substrate concentration.

254 The M^{pro} and PL^{pro} were assayed for amidolytic activity towards the hydrolysis
255 of the synthetic chromogenic substrates for thrombin (S-2238) and coagulation factor
256 Xa (S-2765). Hydrolysis of S-2238 and S-2765 (0.2 mM final concentration) by M^{pro}
257 (10 nM) and PL^{pro} (10 nM) was determined in 50 mM Tris/HCl, 150 mM NaCl, 10 mM
258 CaCl₂, and 0.1% polyethylene glycol (PEG) 6000, pH 7.5. Substrate hydrolysis was
259 detected using a SpectraMax® ABS Plus equipped with a microplate mixer and heating
260 system. Reactions were recorded continuously at 405 nm for 2 hours at 37 °C.

261

262 *In vitro assays*

263 The Calu-3 cells were infected with multiplicity of infection (MOI) of 0.1 at
264 densities of 2.0×10^5 cells/well for 1 h at 310K in 5 % of CO₂. The cells were washed,
265 and different concentrations of each anticoagulant, atazanavir, or remdesivir were added
266 in Dulbecco's modified Eagle medium (DMEM) with 10% fetal bovine serum (FBS).
267 The concentration for anticoagulants and atazanavir was 0.00, 0.63, 1.25, 2.50, 5.00,
268 and 10.0 µM, while remdesivir was 0.00, 0.0001, 0.001, 0.01, 0.10, 0.50, 1.0, 5.0, and

269 10.0, μM . After 48 h, the supernatants were harvested, and virus titers were quantified
270 by plaque-based assays according to previous publications³⁶⁻³⁸,

271 The cytotoxic assays were conducted in a monolayers of Vero cells (in about 2.0
272 $\times 10^4$ cell/well) treated for 3 days with different concentrations of apixaban,
273 rivaroxaban, dabigatran, atazanavir, or remdesivir (50, 150, 300, 600, and 800 μM)
274 following procedure described by Sacramento, C.Q. et al³⁷. The plates were read in
275 terms of absorption in a spectrophotometer at 595 nm and the 50% cytotoxic
276 concentration (CC_{50}) was calculated by a non-linear regression analysis from a dose–
277 response curve.

278

279 *Statistics*

280 All in vitro data were analyzed from Prism GraphPad software 8.0 (Windows
281 GraphPad Software, San Diego, California USA). At least triplicate experiments were
282 performed for each data point, and the value was presented as mean \pm standard
283 deviation (SD).

284

285 *Molecular docking procedure*

286 The crystallographic structure for M^{pro} was obtained from Protein Data Bank,
287 with access code 7K40. The chemical structure for the anticoagulants and M^{pro} substrate
288 used in the experimental assays was built and minimized in terms of energy by Density
289 Functional Theory (DFT) via Spartan'18 software (Wavefunction, Inc., Irvine, CA,
290 USA). The molecular docking calculations were performed with GOLD 2020.2
291 software (Cambridge Crystallographic Data Center Software Ltd., CCDC) at pH 7.4.
292 Redocking studies were carried out with the crystallographic ligand boceprevir
293 (GC376), obtaining the lowest RMSD value by ChemPLP function. The main binding
294 pockets for drugs into M^{pro} were calculated by the free access software from Proteins
295 Plus (Zentrum für Bioinformatik, Universität Hamburg, Germany). It was defined 8 Å
296 radius around each main binding pockets and the figures of the best results were
297 generated with PyMOL Delano Scientific LLC software (DeLano Scientific LLC: San
298 Carlos, CA, USA).

299

300

301 **References**

- 302 **1.** Wu, F. et al. A new coronavirus associated with human respiratory disease in China.
303 *Nature* **579**, 265-269 (2020).
- 304 **2.** WHO coronavirus (COVID-19) dashboard (WHO.INT, 2021)
305 <https://covid19.who.int/>
- 306 **3.** Iba T. et al. Subcommittee on disseminated intravascular coagulation. Differential
307 diagnoses for sepsis-induced disseminated intravascular coagulation: communication
308 from the SSC of the ISTH. *J Thromb. Haemost.* **17**, 415-419 (2019).
- 309 **4.** Connors, J.M., Levy, J.H. COVID-19 and its implications for thrombosis and
310 anticoagulation. *Blood* **135**, 2033-2040 (2020).
- 311 **5.** Ackermann, M.; et al. Pulmonary vascular endothelialitis, thrombosis, and
312 angiogenesis in Covid-19. *New Engl. J. Med.* **383**, 120-128 (2021).
- 313 **6.** Liu, P.P. et al. The science underlying COVID-19: Implications for the
314 cardiovascular system. *Circulation* **142**, 68-78 (2020).
- 315 **7.** Wichmann, D. et al. Autopsy findings and venous thromboembolism in patients with
316 COVID-19. *Ann Intern Med.* M20-2003 (2020).
- 317 **8.** Hottz, E.D. et al. Platelet activation and platelet-monocyte aggregate formation
318 trigger tissue factor expression in patients with severe COVID-19. *Blood* **136**, 1330–
319 1341 (2020).
- 320 **9.** Magro, C. et al. Complement associated microvascular injury and thrombosis in the
321 pathogenesis of severe COVID-19 infection: A report of five cases. *Transl. Res.* **220**, 1-
322 13 (2020).
- 323 **10.** Komiyama, M., Hasegawa, K. Anticoagulant therapy for patients with coronavirus
324 disease 2019: Urgent need for enhanced awareness *Europ. Cardiol. Rev.* **15** e58 (2020).
- 325 **11.** Tiwari, N.R., Khatib, K.I., Dixit, S.B. Anticoagulation in COVID – 19: An update.
326 *J. Crit. Care Med* **6**, 217-223 (2020).
- 327 **12.** Chowdhury, J.F. Anticoagulation in hospitalized patients with Covid-19. *New Engl.*
328 *J. Med.* **383**, 1675-1678 (2020).
- 329 **13.** Flumignan, R.L.G. et al. Prophylactic anticoagulants for people hospitalized with
330 COVID-19. *Cochrane Database Syst. Rev.* **10**, CD013739 (2020).
- 331 **14.** COVID-19 Treatment Guidelines (NIH.USA, 2021)
332 <https://www.covid19treatmentguidelines.nih.gov/therapies/antithrombotic-therapy/>

- 333 **15.** Wenzler, E. et al. Safety and efficacy of apixaban for therapeutic anticoagulation in
334 critically ill ICU patients with severe COVID-19 respiratory disease. *TH Open* **4**, e376–
335 e382 (2020).
- 336 **16.** Adam, Cuker. et al. American Society of Hematology 2021 guidelines on the use of
337 anticoagulation for thromboprophylaxis in patients with COVID-19. *Blood Adv* **5**, 872–
338 888 (2021).
- 339 **17.** Know, C.S., Hasan, S.S. Pharmacologic therapeutic options for thromboprophylaxis
340 in COVID-19. *J. Thromb. Thrombolysis*. 1–2 (2020).
- 341 **18.** Billett, H.H. et al. Anticoagulation in COVID-19: Effect of enoxaparin, heparin, and
342 apixaban on mortality. *Thromb Res.* **120**, 1691-1699 (2020).
- 343 **19.** Orsi, F.A. et al. Guidance on diagnosis, prevention and treatment of
344 thromboembolic complications in COVID-19: a position paper of the Brazilian Society
345 of Thrombosis and Hemostasis and the Thrombosis and Hemostasis Committee of the
346 Brazilian Association of Hematology, *Hematol. Transfus. Cell Ther.* **42**, 300–308
347 (2020).
- 348 **20.** Rossi, F.H. Venous thromboembolism in COVID-19 patients. *J. Vasc. Bras.* **19**,
349 e20200107 (2020).
- 350 **21.** Spyropoulos, A.C. et al. Improved benefit risk profile of rivaroxaban in a
351 subpopulation of the MAGELLAN study. *Clin. Appl. Thromb. Hemost.* **25**, 1-9 (2019).
- 352 **22.** Fischer, A. et al. Computational selectivity assessment of protease inhibitors against
353 SARS-CoV-2. *Int. J. Mol. Sci.* **22**, 2065 (2021).
- 354 **23.** Biembengut, Í.V., de Souza, T.A.C.B. Coagulation modifiers targeting SARS-CoV-
355 2 main protease Mpro for COVID-19 treatment: an in silico approach. *Mem. Inst.*
356 *Oswaldo Cruz* **115**, e200179 (2020).
- 357 **24.** El-Baba, T.J. et al. Allosteric inhibition of the SARS-CoV-2 main protease –
358 insights from mass spectrometry-based assays. *Angew. Chem. Int. Ed. Engl.* **59**, 23544–
359 23548 (2020).
- 360 **25.** Douangamath, A. et al. Crystallographic and electrophilic fragment screening of the
361 SARS-CoV-2 main protease. *Nature Comm.* **11**, 5047 (2020).
- 362 **26.** Chu, H. et al. Comparative tropism, replication kinetics, and cell damage profiling
363 of SARS-CoV-2 and SARS-CoV with implications for clinical manifestations,
364 transmissibility, and laboratory studies of COVID-19: an observational study. *Lancet*
365 *Microbe* **1**, e14–23 (2020).

- 366 **27.** Merad, M. et al. Pathological inflammation in patients with COVID-19: a key role
367 for monocytes and macrophages. *Nature Rev. Immunol.* **20**, 355–362 (2020)
- 368 **28.** Bonaventura, A. et al. Endothelial dysfunction and immunothrombosis as key
369 pathogenic mechanisms in COVID-19. *Nature Rev. Immunol.* **21**, 319–329 (2021).
- 370 **29.** Brown, P.C. Apixaban - Pharmacology/Toxicology NDA review and evaluation.
371 Department of Health and Human Services, Public Health Service, Food and Drug
372 Administration, Center for Drug Evaluation and Research. (2012)
- 373 **30.** He, K. et al. Preclinical pharmacokinetics and pharmacodynamics of apixaban, a
374 potent and selective factor Xa inhibitor. *Eur. J. Drug Metab. Pharmacokinet.* **36**, 129-
375 139 (2011).
- 376 **31.** Rentsch, C.T. et al. Early initiation of prophylactic anticoagulation for prevention of
377 coronavirus disease 2019 mortality in patients admitted to hospital in the United States:
378 cohort study. *British Med. J.* **372**, n311 (2021)
- 379 **32.** de Luca, F.A. et al. Pulmonary embolism in patients with Covid-19 in direct oral
380 anticoagulant. *Int. J. Cardiovasc. Sci.* (2021)
- 381 **33.** Weglarz-Tomczak, E. et al. Ebselen as a highly active inhibitor of PLProCoV2.
382 *bioRxiv* (2020).
- 383 **34.** Liu, W. et al. Learning from the past: possible urgent prevention and treatment
384 options for severe acute respiratory infections caused by 2019-nCoV. *ChemBiochem* **21**,
385 730-738 (2020).
- 386 **35.** Zhang, L. et al. Crystal structure of SARS-CoV-2 main protease provides a basis for
387 design of improved α -ketoamide inhibitors. *Science* **368**, 409-412 (2020).
- 388 **36.** Fintelman-Rodrigues, N. et al. Atazanavir, alone or in combination with ritonavir,
389 inhibits SARS-CoV-2 replication and proinflammatory cytokine production.
390 *Antimicrob. Agents Chemother.* **64**, e00825-20 (2020).
- 391 **37.** Sacramento, C.Q. et al. In vitro antiviral activity of the anti-HCV drugs daclatasvir
392 and sofosbuvir against SARS-CoV-2, the aetiological agent of COVID-19 *J.*
393 *Antimicrob. Chemother.* **76**, 1874–1885 (2021).
- 394 **38.** Puhl, A.C. et al. Repurposing the ebola and marburg virus inhibitors Tilorone,
395 quinacrine, and pyronaridine: In vitro activity against SARS-CoV-2 and potential
396 mechanisms. *ACS Omega* **6**, 7454–7468 (2021).
- 397
- 398
- 399

400 **Acknowledgements**

401 The authors thank the Brazilian agencies for the financial support: Conselho
402 Nacional de Desenvolvimento Científico e Tecnológico (CNPq), and Fundação Carlos
403 Chagas Filho de Amparo à Pesquisa do Estado do Rio de Janeiro (FAPERJ). This study
404 was financed in part by Coordenação de Aperfeiçoamento de Pessoal de Nível Superior
405 (CAPES, Brazil) with finance code 001.

406

407 **Authors contribution**

408 T.M.L.S., H.C.C.-F.-N., and P.T.B. idealized the work. O.A.C., C.Q.S., N.F.-R.,
409 and J.R.T. conducted the SARS-CoV-2 inhibition in Calu-3 cells. O.A.C., F.P.-D., and
410 L.V. conducted the experimental proteases assays. O.A.C. conducted the cytotoxic
411 assays and molecular docking calculations. D.M.M. and R.Q.M. conducted the pro-
412 clotting coagulation assays. O.A.C., R.Q.M., P.T.B., H.C.C-F-N., and T.M.L.S.
413 manuscript preparation.

414

415 **Competing interests**

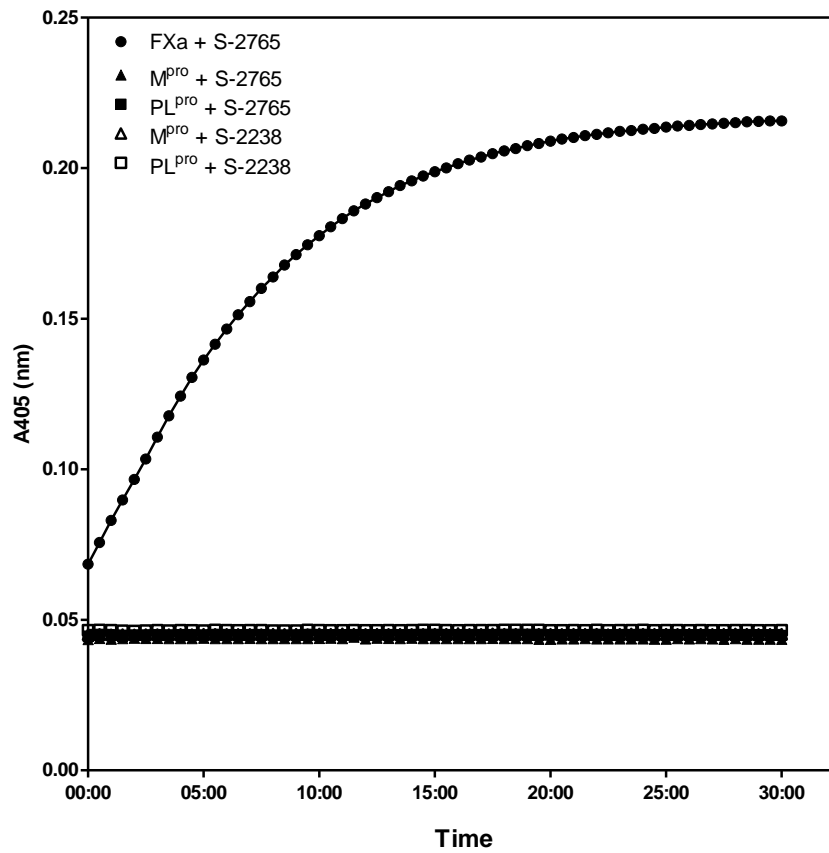
416 The authors declare no competing interests.

417

418

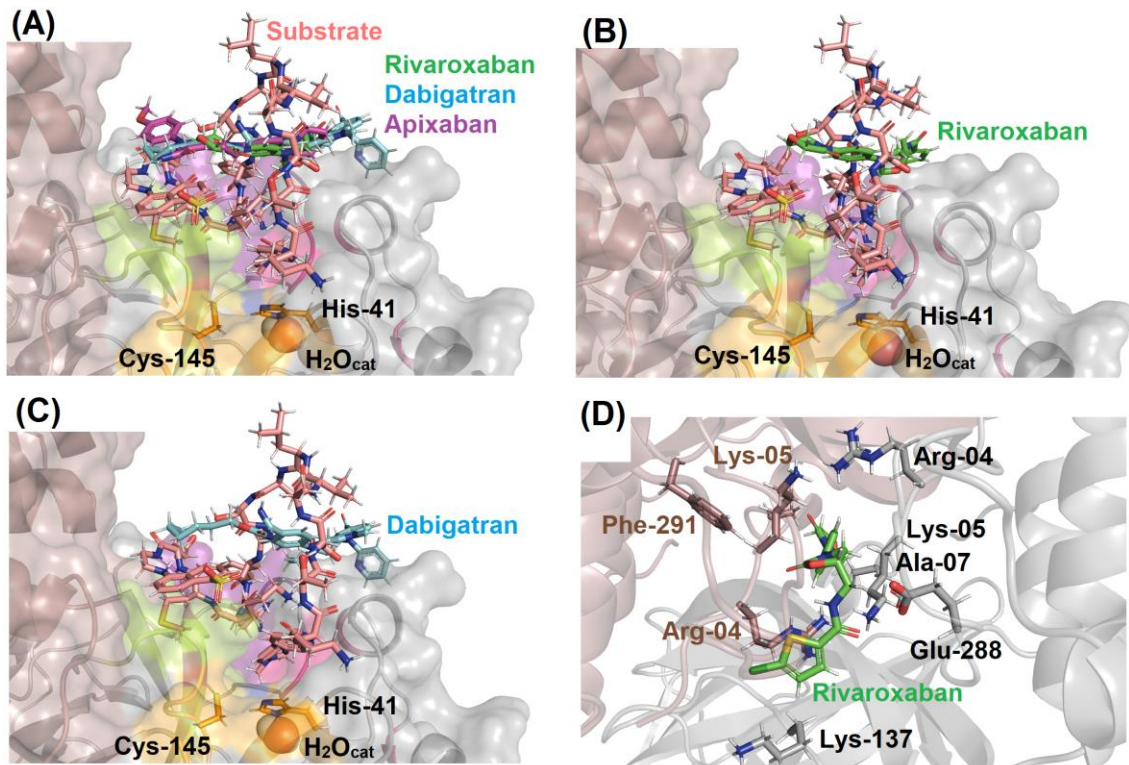
419

Supplementary Information



420

421 **Supplementary Fig. 1.** Cleavage of chromogenic substrates S-2765 and S-2238 by M^{pro} and PL^{pro}. M^{pro}
422 (10 nM) and PL^{pro} (10 nM) were incubated with S-2765 or S-2238 (0.2 mM final concentration) and the
423 kinetic of the reactions was monitored by measuring the absorbance at 405 nm for thirty minutes at room
424 temperature. (●) indicate control performed in the presence of FXa (1.25 nM). Results are expressed as
425 mean values ± SEM of duplicates.



426

427 **Supplementary Fig. 2.** Best docking pose (ChemPLP function) for the interaction between M^{Pro} (A)
428 substrate-anticoagulants, (B) substrate-rivaroxaban, and (C) substrate-dabigatran into the active site of
429 protease. (D) Best docking pose (ChemPLP function) for the interaction between rivaroxaban into the
430 dimer interface M^{Pro}. Substrate, rivaroxaban, dabigatran, and apixaban are in stick representation in beige,
431 green, cyan, and pink, respectively, while the catalytic water (H₂O_{cat}) is in sphere. Elements' color:
432 hydrogen, nitrogen, oxygen, sulfur, and chloro are in white, dark blue, red, yellow, and dark green,
433 respectively.

434

435